Anisotropic waveform inversion gradient from the isotropic wave-equation

Júlio Oliva Frigério, Petrobras, Brazil

Jessé Carvalho Costa, Universidade Federal do Pará, Brazil

This paper was prepared for presentation at the 14th International Congress of the Brazilian Geophysical Society, held in Rio de Janeiro, Brazil, August 3-6, 2015.

Abstract

This paper deals with the use of causality to help filling the null space of linear operators characterizing practical seismic problems as compensation of source and receiver ghosts and absorption. A mathematical approach to the problem is presented followed by some synthetic examples that makes it clear the limitations of this approach and points to new strategies to deal with the inherent uncertainties on the process model parameters.

Introduction

Waveform inversion (WI) is a process to estimate subsurface wave propagation velocity models by iteratively refining a given initial velocity model. At each iteration an update direction is computed from the gradient of the misfit function bewteen field and synthetic data. For pseudo-acoustic anisotropic models, computing the gradient of objective function requires at least three wavefield reconstructions (forward problem), which is computationally demanding in 3D applications.

We present a way for computing the gradient for WI of pseudo-acoustic models using the strategy presented by Alkhalifah, 2013. In this strategy an effective isotropic acoustic medium is used to propagate wavefields with the same traveltime of wavefields propagated in the associated anisotropic medium. The parameters of the isotropic effective medium are derived from the parameters of the anisotropic medium through the solution of the anisotropic eikonal equation. This technique can reduce the cost of anisotropic WI at least four times when compared to efficient methods to solve the pseudo-acoustic anisotropic wave-equation, as the one presented by Fowler, Du & Fletcher (2010).

Theory

The works of da Silva & Sava(2009) introduced the concept of kinematically equivalent isotropic media in the context of migration of common-offset data. The solution to the isotropic eikonal equation in the equivalent medium reproduces the isochrons of the migration impulse response for finite offset data. Alkhalifah et al., 2013, showed that this concept can be extended to anisotropic models and presented its application to RTM in TTI models, demonstrating that it is possible to build an effective isotropic model in which the wavefronts present the same traveltimes of the wavefield in the original anisotropic model. This construction is valid for anisotropic media with all kinds symmetry.

If a TTI medium is considered, this concept can be mathematically expressed as follows. Let the anisotropic parameters of the original model be:

$$m_{ani} = \{\, v_0(\vec{x}),\ \varepsilon(\vec{x}),\ \delta(\vec{x}),\ \theta(\vec{x}),\ \phi(\vec{x}) \,\} \tag{1}$$

The effective isotropic model is parameterized by:

$$m_{iso} = \{\, v_{eff}(\vec{x}) \,\} \tag{2}$$

The condition to build the effective model is that the traveltime of first arrivals are equal in both models:

$$\tau_{iso}(\vec{x}; v_{eff}) = \tau_{ani}(\vec{x}; v_0, \varepsilon, \delta, \theta, \phi) = \tau(\vec{x}) \tag{3}$$

Hence, there is a functional relation between the parameters of m_{ani} and m_{iso}:

$$v_{eff}(\vec{x}) = \zeta(\, v_0(\vec{x}),\ \varepsilon(\vec{x}),\ \delta(\vec{x}),\ \theta(\vec{x}),\ \phi(\vec{x}) \,) \tag{4}$$

The relation of equation 4 can be established in the following way. First we compute the traveltimes $\tau(\vec{x})$ by solving the anisotropic eikonal equation for a point source in the original medium:

$$H_{ani}(\vec{p}; v_0, \varepsilon, \delta, \theta, \phi) = 0, \tag{5}$$

where

$$H_{ani} \equiv c_\varepsilon[\vec{p}\cdot\vec{p} - (\vec{p}\cdot\hat{n})^2] + c_0(\vec{p}\cdot\hat{n})^2 - c_0(c_\varepsilon - c_\delta)[\vec{p}\cdot\vec{p} - (\vec{p}\cdot\hat{n})^2](\vec{p}\cdot\hat{n})^2 - 1 \tag{6}$$

$$c_0 = v_0^2 c_\varepsilon = v_0^2(1+2\varepsilon) c_\delta = v_0^2(1+2\delta) \vec{p}(\vec{x}) = \nabla\tau(\vec{x}) \tag{7}$$

In the equations above, $\vec{p}(\vec{x})$ is the slowness at the point $\vec{x}$. Then, we use the computed traveltime/slowness to solve the isotropic eikonal for the effective parameter c_{eff}:

$$H_{iso}(\vec{p}; c_{eff}) = 0, \tag{8}$$

where

$$H_{iso} \equiv \frac{1}{2}\left[c_{eff}\,(\vec{p}\cdot\vec{p}) - 1\right] \tag{9}$$

$$c_{eff} = v_{eff}^2 \tag{10}$$

Finally, the parameter $c_{eff}(\vec{x})$ defines the effective isotropic model and can be used to compute a wavefield with the acoustic wave-equation:

$$\nabla^2\psi(t,\vec{x}) - \frac{1}{c_{eff}}\frac{\partial^2\psi(t,\vec{x})}{\partial t^2} = s(t)\,\delta(\vec{x} - \vec{x}_0), \tag{11}$$

where $s(t)$ is the point source time function.

The effective model is built in a way that traveltimes are correct, but the same is not guaranteed for the amplitudes of the wavefield. For this reason, the functional we choose for the local optimization process should preferrably be more sensitive to traveltimes. One functional that satisfies this requirement is that proposed by Luo and Schuster, 1991. It is defined in the following way:

$$\Phi = \sum_{s,r} \Delta\tau_{s,r}^2, \tag{12}$$

where the indexes s and r designate a source and a receiver station, respectively. The quantity $\Delta\tau_{s,r}$ is defined by means of the connective function $f_{s,r}(\tau)$, which is the normalized cross-correlation between synthetic and observed data:

$$f_{s,r}(\tau) = \int dt\ \frac{d_{s,r}^{obs}(t+\tau)\ d_{s,r}^{syn}(t)}{A_{s,r}^{obs}}, \tag{13}$$

where $A_{s,r}^{obs}$ is the absolute value of the maximum amplitude of $d_{s,r}^{obs}$. We define $\Delta\tau_{s,r}$ as the lag for which $f_{s,r}$ reaches its maximum value:

$$f_{s,r}(\Delta\tau_{s,r}) = max\{f_{s,r}(\tau)\} \tag{14}$$

As $\Delta\tau_{s,r}$ depends on the model parameters, Φ does too. Moreover, the dependence on the anisotropic parameters is given indirectly through the effective parameter c_{eff}:

$$\Phi = J(\,c_{eff}(c_0,\,c_\varepsilon,\,c_\delta)\,) \tag{15}$$

In equation 15, the dependence of the objective function J on the angular anisotropic parameters θ and ϕ can be ignored if we assume that these parameters are given a priori. As a matter of fact, even though we are writing equations 1 through 15 for a TTI model, it is straightforward to write them for any kind of anisotropic model.

As a consequence of the indirect dependence expressed in equation 15, the gradient of J with respect to the anisotropic parameter c_i is given by the following chain rule for derivatives:

$$\nabla_{c_i} J = (\nabla_{c_{eff}} J) \cdot \frac{\partial c_{eff}}{\partial c_i} \tag{16}$$

As shown by Luo & Schuster (1999), Pratt, Shin & Hicks (1998), and Tarantola (1984), the gradient $\nabla_{c_{eff}} J$ is the the zero-lag of the time correlation between the back-propagated residuals and the second time-derivative of the source wavefield.

The partial derivatives $\partial c_{eff}/\partial c_i$ can be computed by means of the isotropic and anisotropic eikonals as follows. Considering the stationarity of the Hamiltonians H_{iso} and H_{ani} (equations 6 and 9), we may write:

$$\frac{dH_{ani}}{dc_i} = \nabla_{\vec{p}} H_{ani} \cdot \frac{\partial \vec{p}}{\partial c_i} + \frac{\partial H_{ani}}{\partial c_i} = 0 \tag{17}$$

As $\vec{p} = p\hat{n}$, where $\hat{n}$ is the ray direction, we have:

$$\frac{dH_{ani}}{dc_i} = \nabla_{\vec{p}} H_{ani} \cdot \left(\frac{\partial p}{\partial c_i}\,\hat{n} + p\,\frac{\partial \hat{n}}{\partial c_i} \right) + \frac{\partial H_{ani}}{\partial c_i} = 0 \tag{18}$$

Variations in c_i should have a significant impact on the direction of the ray only in the second order. In this case, we may neglect $\partial\hat{n}/\partial c_i$. Equivalently for the isotropic Hamiltonian:

$$\frac{dH_{iso}}{dc_i} = \nabla_{\vec{p}} H_{iso} \cdot \frac{\partial \vec{p}}{\partial c_i} + \frac{\partial H_{iso}}{\partial c_{eff}} \cdot \frac{\partial c_{eff}}{\partial c_i} = 0 \tag{19}$$

Neglecting $\partial\hat{n}/\partial c_i$ and considering that $p = 1/v_{eff}$:

$$\frac{dH_{iso}}{dc_i} = v_{eff}\,\frac{\partial p}{\partial c_i} + \frac{\partial H_{iso}}{\partial c_{eff}} \cdot \frac{\partial c_{eff}}{\partial c_i} = 0 \tag{20}$$

Replacing $\partial p/\partial c_i$ in equation 18 from equation 20 and observing that $\vec{p} \cdot \nabla_{\vec{p}} H_{ani} = 1$, we end up with:

$$\frac{\partial c_{eff}}{\partial c_i} \approx c_{eff}\,\frac{\partial H_{ani}}{\partial c_i} \tag{21}$$

Substituting equation 21 in equation 16:

$$\nabla_{c_i} J \approx (\nabla_{c_{eff}} J) \cdot c_{eff}\,\frac{\partial H_{ani}}{\partial c_i} \tag{22}$$

Synthetic Experiment

As a proof of concept, we designed a computational experiment in which we apply the method described above. In this experiment we generate synthetic data from a VTI model with homogeneous background and two gaussian anomalies (figure). The background values of the anisotropic parameters are: $v_0 = 1500.0\,m/s,\ \varepsilon = 0.0,\ \delta = 0.0$. In this experiment shot points are placed on the surface (above) and receivers are placed underneath the anomalies. This configuration of shot and receiver points provides illumination of the anomalies with a wide and relatively homogeneous range of angles, which favours analisys of the gradient built with the method presented above.

Figure 2 shows the partial derivatives $\partial c_{eff}/\partial c_i$ for a shot point at the middle of the model's upper boundary. Red-coloured regions possess high values of derivatives and correspond to locations where the effective parameter c_{eff} is more sensitive to that specific anisotropic parameter. The patterns we see are consistent with what is expected for each anisotropic parameter. In other words, c_{eff} is more sensitive to the squared vertical velocity c_0 along wavepaths close to the vertical direction; c_{eff} is more sensitive to the squared horizontal velocity c_ε along wavepaths close to the horizontal direction; c_{eff} is more sensitive to the squared moveout velocity c_δ along wavepaths close to intermediate directions (45 degrees).

Finally, figure 3 shows the isotropic gradient above the anisotropic gradients for c_0 and c_ε. Displayed on top is the representation of the model with the gaussian anomalies. From the figure one can realize that the isotropic gradient recovers in c_{eff} both anomalies. The anisotropic gradient for c_ε presents strong cross-talk and contains high amplitudes in the location of the c_0 anomaly. On the other hand, the gradient for c_0 is less sensitive to cross-talk and presents high amplitudes only in the location of the c_0 anomaly. This is in accordance with the ideas discussed by Operto et al (2013) about multiparameter FWI. The recomendations given by them in the paper should be followed here: inversion for c_0 must be performed first, after which the inversion can be done for the anisotropic parameter c_ε. Another way of reducing cross-talk between parameters is by applying the inverse of the hessian operator. Further work will demonstrate how to perform the computation of the Hessian and how to apply its inverse.

Conclusion

We presented a new method for computing the gradient for anisotropic waveform inversion using the concept of kinematically equivalent isotropic medium. Since this method requires only the solution of the acoustic wave-equation, it is at least four times more efficient than methods using pseudo-acoustic wave-equations, and at least one order of magnitude more efficient than methods based on the solution of anisotropic elastic wave-equation. The restriction here is that only first arrivals are used in the inversion. Hence, it is more suitable for shallow zones or regions with a depth increasing velocity gradient.

References

Alkhalifah, T., X. Ma, U. bin Waheed, M. Zuberi, 2013, Efficient anisotropic wavefiled extrapolation using effective isotropic models: International Congress of the Brazilian Geophysical Society.

Fowler, P. J., X. Du, R. P. Fletcher, 2010, Coupled equations for reverse time migration in transversely isotropic media: Geophysics, 75, S11-S22.

Luo, Y., G. T. Schuster, 1991, Wave-equation traveltime inversion, Geophysics: 56, 645-653.

Operto, S., Y. Gholami, V. Prieux, A. Ribodetti, R. Brossier, L. Meltivier, J. Virieux, A guided tour of multiparameter full -waveform inversion with multicomponent data: From theory to practice: The Leading Edge, 32, 1040-1054 Pratt, R. G., C. Shin, and G. J. Hicks, 1998, Gauss-Newton and full Newton methods in frequency-space seismic waveform inversion: Geophysical Journal International, 133, 341-362.

da Silva, E. F. F., P. C. Sava, 2009, Modeling and migration with orthogonal isochron rays: Geophysical Prospecting, 57, 773-784.

Tarantola, A., 1984, Inversion of reflection seismic data in the acoustica approximation: Geophysics, 49, 1259-1266.

Acknowledgments

The authors express their gratitude to Eduardo Filpo Ferreira da Silva for the fruitful discussions on the computation of the effective isotropic model. The authors also would like to thank Petrobras and Universidade Fedral do Pará for supporting their work and providing resources for its execution. Last but not least, the authors are grateful for the lifelong support from their families.

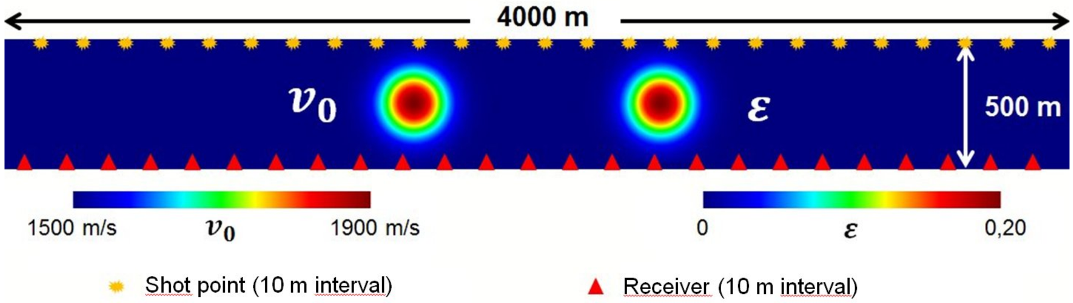

Figure 1: *Synthetic experiment with homogeneous background and gaussian anomalies in vertical velocity v_0 (left anomaly) and in ε (right anomaly). Shot points are located on the surface and receivers are placed underneath the anomalies.*

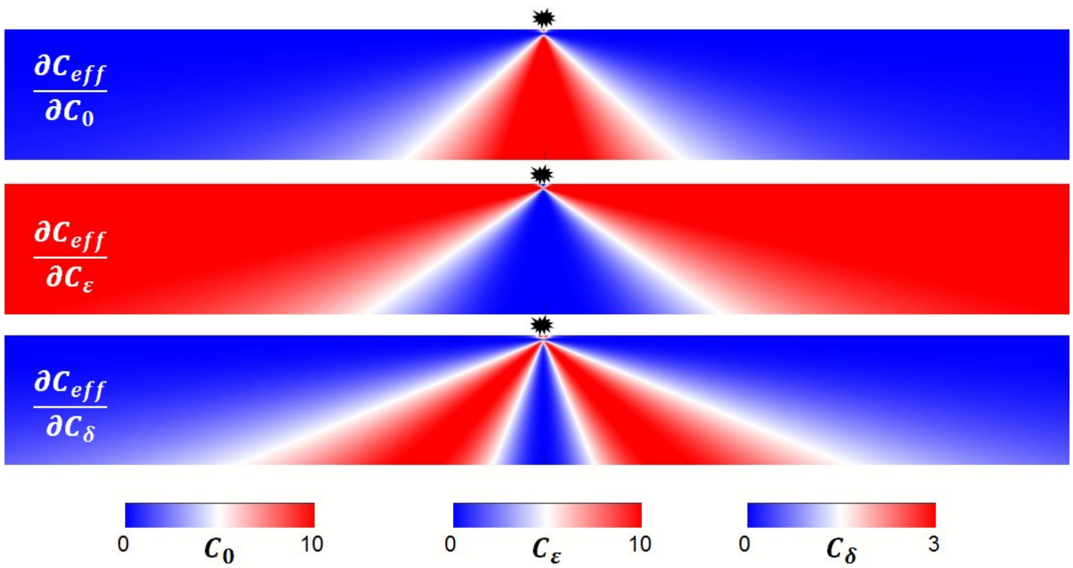

Figure 2: *From top to bottom partial derivatives for: c_0, c_ε and c_δ.*

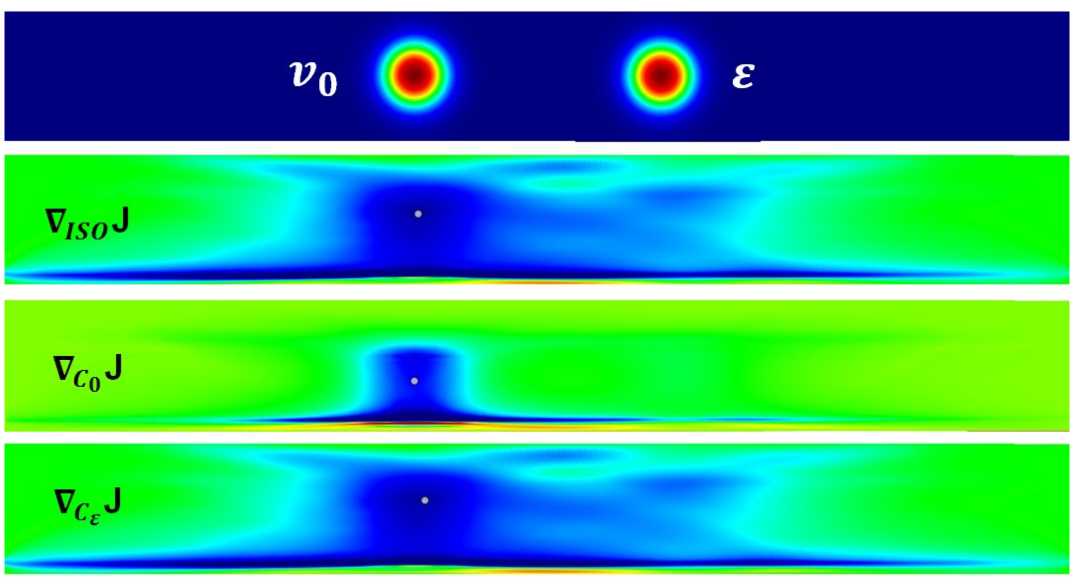

Figure 3: *From top to bottom: Representation of the model and the gaussin anomalies in c_0 and in c_ε; isotropic gradient; gradient for parameter c_0; gradient for parameter c_ε.*